Comparative Study of the Hydrolysis of Different Oils by Lipase-Immobilized Membranes

S. Gupta, P. Ingole, K. Singh, A. Bhattacharya

Reverse Osmosis Discipline, Central Salt and Marine Chemicals Research Institute, Council of Scientific and Industrial Research, G. B. Marg, Bhavnagar 364002, Gujarat, India

Received 19 November 2010; accepted 26 July 2011
DOI 10.1002/app.35400
Published online 29 November 2011 in Wiley Online Library (wileyonlinelibrary.com).

ABSTRACT: Lipase immobilization on asymmetric polysulfone (PS) membranes was done by physical adsorption and covalent coupling techniques. The glutaraldehyde (Glu) crosslink showed maximum immobilization (1.53 mg/cm^2) on the hydrazine (Hz)-modified membrane surface. Lipase immobilization on the membrane was proved by different analytical tools (viz., X-ray diffraction, scanning electron microscopy). The hydrolase-immobilized enzyme marked its hydrolyzing ability to different oils (olive, palm, and castor oils). The hydrolysis yield (U/mg) for the different immobilized membranes was in the following order: Olive oil > Palm oil > Castor oil. The PS–Hz–Glu–lipase membrane showed maximum hydrolyzing ability for olive oil (62.37 U/mg) and minimum hydrolyzing ability for castor oil (38.11 U/mg). The low aptitude for the hydrolysis of castor oil was explained by the presence of ricinoleic acid in the main composition. The lowest affinity toward castor oil (Michaelis–Menten constant = 18.86 m*M*) also featured the same. The order of maximum reaction rate for the same membrane was as follows: Olive oil (64.5) > Palm oil (62.5) > Castor oil (41.6). The immobilized lipase on PS–Hz–Glu suffered only a 12.5% deterioration for olive oil after five cycles. © 2011 Wiley Periodicals, Inc. J Appl Polym Sci 124: E17–E26, 2012

Key words: catalysts; enzymes; irradiation; membranes; surface modification

INTRODUCTION

To overcome the limitations of chemical catalysts in terms of low specificity, purity of the products without further purification steps, and high temperature requirements, biocatalysts are preferred. Enzymes are biocatalytic active entities facilitate chemical and biochemical reactions by lowering the energy of activation of the reactants.[1] Thus, enzyme-catalyzed processes are an alternative route to compete with conventional chemical synthesis. The activities of glucose oxidase (oxidation of glucose), urease (urea hydrolysis), lipase (oil hydrolysis, interesterfication of oils), protease (protein hydrolysis), and amylase (to degrade starch) are well known. To make it cost effective, in one approach, the enzyme needs to be bound on a solid support (i.e., immobilized) so that it can be reused a number of times.[2–4] The target of immobilizing enzymes is to restrict their mobility over solid matrices without losing their activities.[5] Noinville et al.[6] showed that lipases in immobilized condition are in open form, that is, without lids and capable of showing better activities.

Several techniques (viz., adsorption, entrapment, covalent coupling) have been reported in the literature to immobilize enzymes on solid supports.[7–10] Although it depends on the feasibility, covalent coupling is favored as the desorption of enzymes can be avoided compared to other techniques, and as a result, the reusability feature is improved. The large surface area and ease of preparation in different geometric configurations and the flexibility to introduce new functional groups makes these membrane systems more attractive.

Lipases, the triacyl glycerol hydrolases (EC 3.1.1.3), are enzymes possessing an intrinsic capacity to catalyze the cleavage of carboxy ester bonds in tri-, di-, and mono- acyl glycerols. They are marked because of their abundance in nature, their chemo-, regio-, and stereoselectivity, their ability to function in aqueous/nonaqueous environments, and their near interfaces.[11–13] *Candida rugosa* lipases are preferred in industrial applications because of their high inherent activity and broad specificity. They are immobilized by covalent coupling and adsorption on asymmetric polysulfone (PS) membranes through the Coulet and glutaraldehyde (Glu) methods. Because the enzymes never come into contact with strong chemical reagents, their activities are not disturbed in the processes.[14] PS is preferred because of its nontoxic, hydrophobic, thermally and chemically resistant nature,[15] and usefulness in food, water, and medical applications.[16–19] Tailor-made specifications

Correspondence to: A. Bhattacharya (bhattacharyaamit1@rediffmail.com).

Contract grant sponsor: Council of Scientific and Industrial Research, India.

in terms of porosity generation in membranes are easy for PS by the simple wet-phase inversion technique.[20] The lipase-immobilized membranes show the potential to catalyze various reactions, namely, hydrolysis, esterification, interesterification, and transesterification. The hydrolysis of oils, that is, the formation of glycerol and fatty acids from triglycerides[6] is the basis for different commercial applications, that is, soap production, synthetic detergents, greases, cosmetics, and several other products.[21,22] Hydrolysis by immobilized membranes is an energy-saving technique and is advantageous over the conventional Colgate–Emery steam hydrolysis process, where fat splitting operates with superheated steam at 250°C and 50 atm of pressure, and alkaline hydrolysis, where the acidification of soaps is needed to produce the fatty acid products.[23–25]

Reports in the literature on immobilization activities have mainly dealt with commercial membranes, where the composition was really not disclosed. In this study, we experimented with our laboratory-made membrane. The membrane modification approaches were also compared in terms of the immobilization of lipases. The hydrolysis experiment was carried out for different oils (viz., olive oil, palm oil, and castor oil). All were basically triglycerides. The usual high-temperature and high-pressure process for manufacturing fatty acids was not suitable for castor oil hydrolysis because of the intermolecular esterification of ricinoleic acid, which results in the formation of estolides.[26] It was our attempt to immobilize lipases onto the membrane by a covalent binding approach and to determine a possible correlation regarding the hydrolysis extent of three oils with their chemistry and also their kinetic parameters, as determined from a Lineweaver–Burk plot.

EXPERIMENTAL

Materials used

C. rugosa lipase (EC 3.1.1.3; Sigma-Aldrich), PS (Udel P-3500, Solvay Advanced Polymer), refined olive oil (SRL, India), and palm oil and castor oil (Shreeji Chemicals, India) were the chemicals on which we focused for these particular experiments. The structures and compositions of the oils are presented in Table I.[27] Nonwoven polyester fabric (Filtration Sciences Corp.), *N,N′*-dimethylformamide (DMF; Qualigen, India), acrylic acid (AA; SRL), hydrazine (Hz; Loba Chemicals, India), and methanol (SRL) were used. Sodium nitrite, hydrochloric acid, and Glu (S. D. Fine Chemicals, India) were used for immobilization. Folin reagent (S. D. Fine Chemicals), disodium tartarate (S. D. Fine Chemicals), and bovine serum albumin fraction V (Sigma-Aldrich) were used for protein estimation. Acacia powder (S. D. Fine Chemicals) and sulfuric acid (SRL) were also procured. Reverse-osmosis-treated water was used in all cases during the experiment.

Methods

Preparation of asymmetric PS membranes

Asymmetric membranes were prepared by a wet-phase inversion technique.[28] PS solution (15% w/w in DMF) was prepared with heating and stirring. The solution was cast with the help of a prototype casting machine in uniform thickness on a nonwoven polyester fabric support and immediately coagulated

TABLE I
Structures and Compositions of the Oils

Oil	Chemical composition	Structure
Palm oil	Palmitic acid: 44.3% Oleic acid: 38.7% Stearic acid: 4.6% myristic acid: 1% Linoleic acid: 10.5%	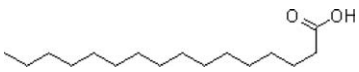 $C_{16}H_{32}O_2$ hexadecanoic acid (palmitic acid)
Olive oil	Oleic acid: 55–83% Palmitic acid: 7.5–20% Linoleic acid: 3.5–21% Stearic acid: 0.5–5% Linolinic acid: >1.5%	 $C_{18}H_{34}O_2$ *cis*-9-Octadecenoic acid (oleic acid)
Castor oil	Ricinoleic acid: 95% Oleic acid: 2% Linoleic acid: 1% Linolinic acid:0.5% Stearic acid: 0.5% Palmitic acid: 0.5% Dihydroxy stearic acid: 0.3%	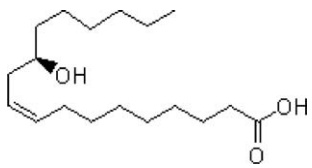 $C_{18}H_{34}O_3$ *cis*-12-hydroxyoctadeca-9-enoic acid (ricinoleic acid)

in a water gelation bath. Sodium lauryl sulfate was added to the gelation bath to control the uniform pores in the membrane. The membranes were kept in the gelation bath for at least 3 h to complete the phase-inversion process. The membranes were washed and stored in water.

Modification of the membranes

AA (1, 5, and 10% v/v in water) solutions were spread on the PS membranes for 10 min. The solution was decanted from the membrane surface and photoirradiated by a UV lamp (HPM-13, 1000 W, Philips, Belgium) for 5 min at ambient temperature. The radiation density flux on all of the membrane surface areas was assumed to be constant in each run. The arrangements were already described in our previous publication.[29]

Immobilization of lipase on the membranes with Hz

PS-*g*-AA membranes were used for the surface covalent binding of lipases. The PS-*g*-AA membranes were first acid-methylated and then activated by acyl azide formation.[30] After the removal of reagents by repeated washing, lipase coupling was performed by immersion of the membranes in the lipase solution (containing 2 mg/mL in 0.1*M* sodium phosphate buffer at pH 7) under standard conditions of 0°C for 4 h. The Glu technique was also employed for immobilization. In this case, acyl azide modified membranes were treated with 2.5% Glu for 4 h before they were dipped in lipase solution, as mentioned before. The same Glu technique for immobilization was also employed for the virgin PS membrane.

Estimation of the amount of lipase immobilized on the membranes:

The amount of immobilized lipase on the membrane was determined by Lowry's method.[31,32] The lipase concentration was determined in accordance with bovine serum albumin as a standard protein. It is mathematically presented as follows:

$$w = (C_1 - C_2)\frac{V}{A} \quad (1)$$

where w is the total immobilized amount (mg/cm^2); C_1 and C_2 are the initial concentrations of the free lipase and decant after immobilization, respectively (mg/mL); V is the reaction volume (mL); and A is the area of the PS membranes (cm^2).

Hydrolytic activities of the free lipase and immobilized membranes

Five milliliters of oil emulsion (oil + gum acacia + Na-benzoate) in 5 mL of phosphate buffer (pH 8) was used for the hydrolytic experiment. The reaction was initiated by the addition of 1 mL of free lipase or with immobilized membranes (6 cm^2). An acetone–methanol (1:1) mixture was added to cease the reaction. The free fatty acid released during the hydrolysis was estimated through 0.01*N* NaOH titration. Lipase assay was performed with olive oil hydrolysis. The same procedure was also followed for palm and castor oil hydrolyses.

Techniques

The quantitative analysis of the immobilized lipase before and after the experiment was done in an indirect manner, that is, from the amount of lipase before and after the experiments. An ultraviolet–visible spectrophotometer (Varian, Carry 500 Scan) was used for the protein estimation.

Fourier transform infrared (FTIR)–attenuated total reflection (ATR) spectroscopy was recorded on a PerkinElmer GX spectrometer with a germanium crystal (refractive index (n_1) = 4.01) with a size of 25 × 5 × 2 mm^3 at a speed of 100 scans, a resolution of ±4 cm^{-1}, and an incident angle of 45°. Thermogravimetric analysis (Metler) studies were done in a nitrogen environment (10°C/min) from 30 to 600°C. CHN analysis (PerkinElmer, series II CHNS/O 2400 analyzer) was done to prove the presence of nitrogen on the membranes after azide formation on the membranes. An X-ray diffractometer (X'PERT, Philips; Cu Kα radiation was the monochromator) and a scanning electron microscope (Leo, 1430UP Oxford Instruments) were used to prove the lipase immobilization on the membrane.

Pure water permeability (PWP) was tested for virgin PS and the modified membranes. PWP of the membranes was tested through crossflow filtration

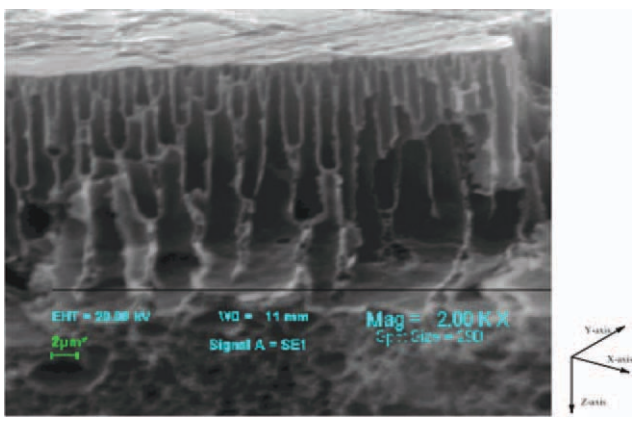

Figure 1 Cross-sectional morphology of the asymmetric PS membrane. The x and y axis denote the top of the membrane, whereas the z axis symbolizes perpendicular to the plane of the film. [Color figure can be viewed in the online issue, which is available at wileyonlinelibrary.com.]

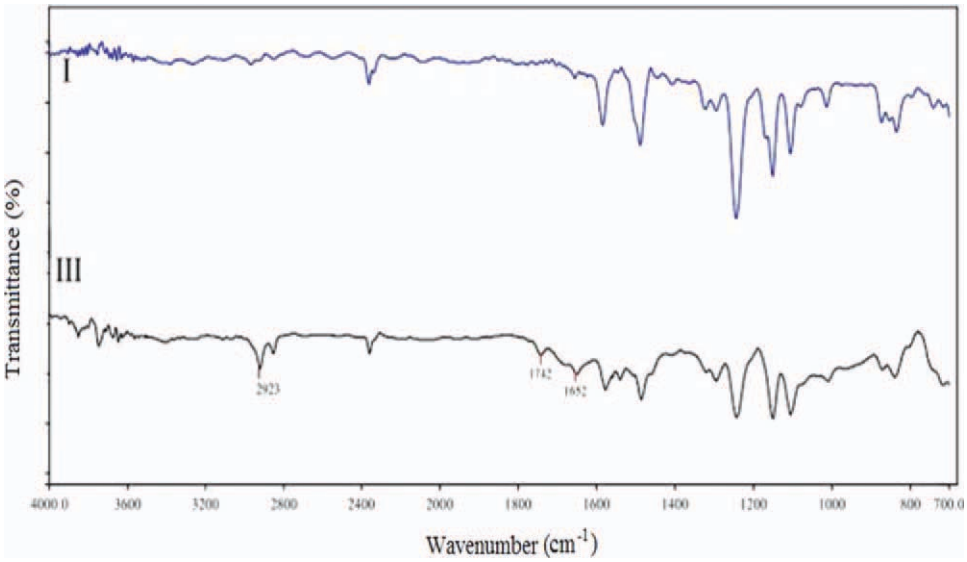

Figure 2 FTIR–ATR spectra of the membranes: (I) virgin PS and (III) PS–AA-II–Hz membrane. [Color figure can be viewed in the online issue, which is available at wileyonlinelibrary.com.]

techniques.[33] A flat, circular shaped membrane with an effective area of 15.2 cm^2 was used for this case. The PWPs of the membranes were recorded after 1 h of pressurization to stabilize the flux at 1.034 MPa of pressure.

The hydrolytic activities for olive oil under optimum conditions (pH 8, temperature = 37°C, reaction time = 30 min) were studied for the reusability study of the three membranes (viz., PS–Hz–Glu–lipase, PS–Glu–lipase, and PS–Azo–lipase). At the end of each batch, the systems were recycled for the next batch. A confirmatory study of reusability was carried out by hydrolysis for the same time intervals (30 min) with a recycled immobilized enzyme.

RESULTS AND DISCUSSION

The PS membrane preparation was done by a wet-phase inversion technique. The diffusion exchange of DMF with water in a coagulation bath occurred, and a homogeneous PS solution underwent phase separation into polymer-rich and polymer-lean

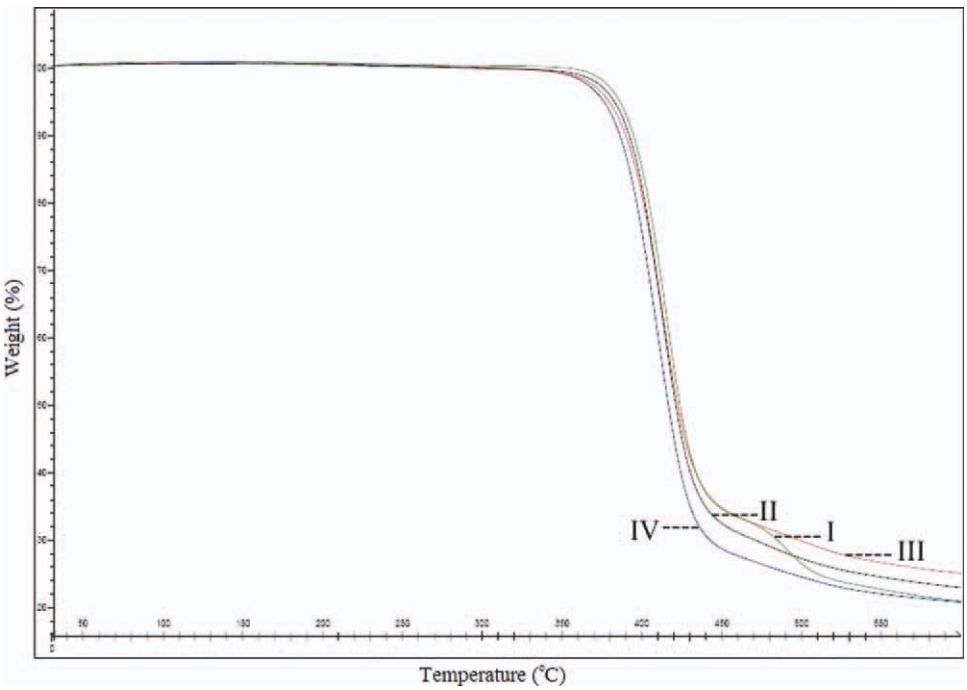

Figure 3 Thermograms of the membranes: (I) virgin PS, (II) PS–(AA)-I–Hz, (III) PS–(AA)-II–Hz, and (IV) PS–(AA)-III–Hz. [Color figure can be viewed in the online issue, which is available at wileyonlinelibrary.com.]

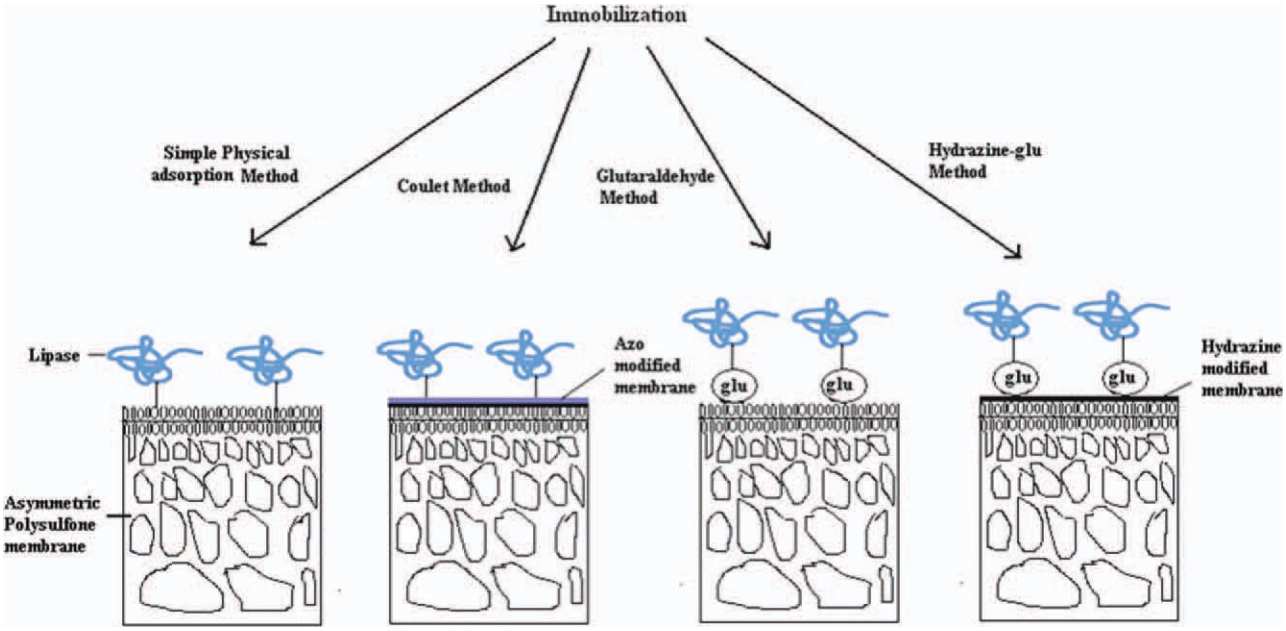

Scheme 1 Different statuses of immobilization by different techniques: (I) physical adsorption, (II) covalent coupling through the Coulet method, (III) adsorption with Glu, and (IV) covalent coupling by Hz–Glu. [Color figure can be viewed in the online issue, which is available at wileyonlinelibrary.com.]

phases. The diffusion exchange of DMF and water across the interface lowered the Gibbs free energy of mixing[34–36] and could make the PS solution phase-separate to form the solid PS. Thus, heterogeneity was developed in the membrane, and it was termed as an *asymmetric membrane*. Asymmetric membranes are favored because of their anchoring feasibility. The polymer-dense phase is on top, and channels and macrovoids are beneath it. The asymmetric nature along the *z* axis perpendicular to the plane of the film is depicted from the cross-sectional morphology (Fig. 1).

The surface functionality of the PS membrane was developed through AA attachment. The photoinduced modification feasibility was with the light absorption by the phenoxyphenyl sulfone chromophore and the cleavage of C—S bonds at the sulfone linkage.[37] The probable mechanism of photoinduced modification was depicted in our earlier experimental study.[29] AA modification was primarily reflected in the weight increase of the modified membranes. The weight increase (range = 10^{-7} mol/cm^2) depended on the AA concentration.

The esterification of the PS-*g*-AA membrane was done by methanol in an acidic condition. Treatment with ester with Hz formed an azide in its functionality, as —OMe was a readily leaving group. C, H, and N analysis showed the presence of nitrogen content in the compound. FTIR–ATR spectra (Fig. 2) showed the evidence of —NH (3750–3600 cm^{-1}), —CONH— (2923 cm^{-1}) of hydrazide, >C=O of amide (1652 cm^{-1}), and —COOMe (1742 cm^{-1}) groups in the azide-modified membrane [Fig. 2(III)]. Thermogravimetric analysis studies also showed a systematic difference in the degradation patterns of the azide-modified membranes (for different AA concentrations; Fig. 3), although it was small. The Coulet and Glu techniques were employed to form the attachment of lipase onto the azide-modified membranes. The different statuses of the immobilizations are depicted in Scheme 1. The physical adsorption of lipase (without and with Glu) occurred in modes I and III of Figure 3, whereas chemical coupling existed in modes II and IV of Figure 3.

In our earlier article,[32] the subject of attention was that the amount of immobilization differed with the nature of the membranes. Only a physical adsorption method was employed. It was evidenced that PS, being more hydrophobic, showed better

TABLE II
Lipase Immobilization Amount on Membranes by Different Methods

	Lipase-immobilized amount (mg/cm^2)	
Membrane	Azo reaction (Coulet method)	Glu treatment after Hz modification
Virgin PS	0.280[a]	1.11[b]
PS–AA-I	0.59	1.41
PS–AA-II	0.76	1.53
PS–AA-III	0.75	1.53

I, II, and III designate 1, 5, and 10% AA.
[a] No treatment.
[b] Only Glu treatment.

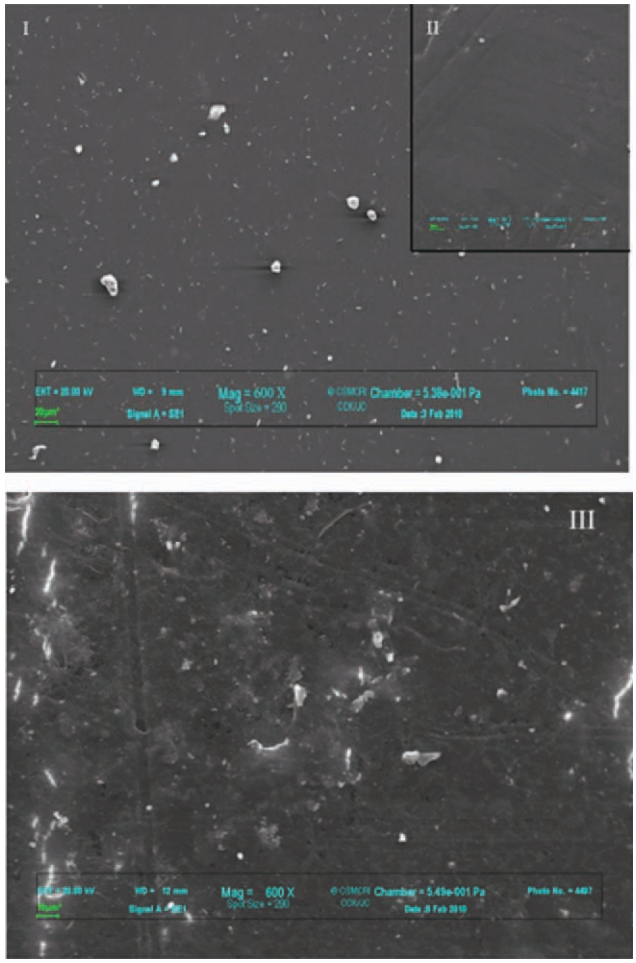

Figure 4 Scanning electron micrograph of the (I) Hz-modified membrane PS–(AA)-II–Hz, (II) the embedded one, virgin PS, and (III) lipase-immobilized membrane (PS–AA-II–Hz) with the Glu technique. [Color figure can be viewed in the online issue, which is available at wileyonlinelibrary.com.]

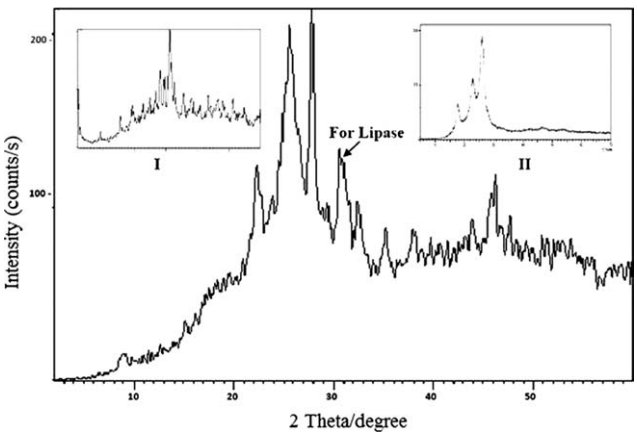

Figure 5 XRD pattern of the lipase-immobilized PS membrane (PS–AA-II–Hz) with the Glu technique: Inset I shows the free lipase powder and inset II shows the polyester fabric.

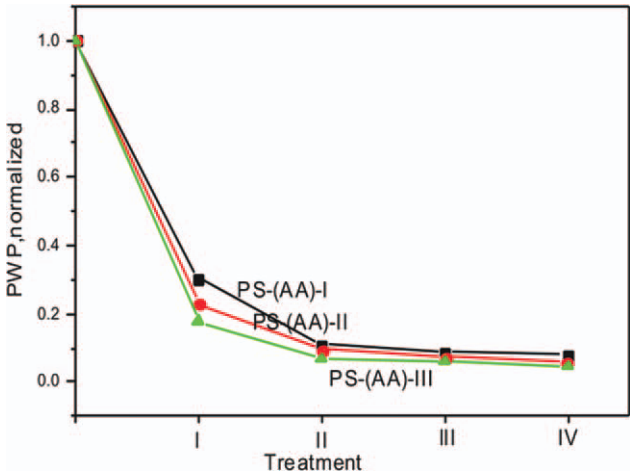

Figure 6 Normalized PWP for the modified membranes with different modification stages: after (I) AA grafting, (II) methanol treatment, (III) Hz treatment, and (IV) lipase treatment. [Color figure can be viewed in the online issue, which is available at wileyonlinelibrary.com.]

immobilization compared to poly(ether sulfone). In this study, different immobilization techniques were employed. The variation in immobilization amounts of lipase by different techniques was in ensemble (Table II). Adsorption through Glu was greater with respect to physical adsorption on virgin PS. The covalent coupling (i.e., Coulet and Glu methods) showed better results compared to physical adsorption on virgin PS. The immobilization with Glu on the Hz-mediated surface was greater compared to that on the Coulet one, as there were crosslinking chances of lipase units and binding with the azide functionality. The lipase immobilization depended on the azide content and the AA content in both

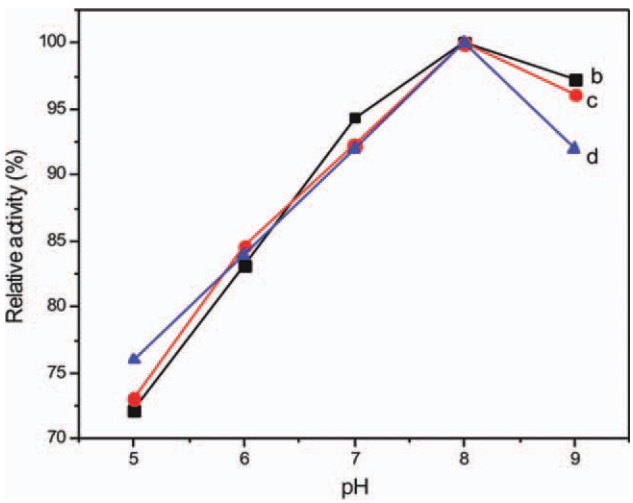

Figure 7 Variation of the relative hydrolytic activity (%) with pH: (b) PS–Hz–Glu–lipase, (c) PS–Glu–lipase, and (d) PS–Azo–lipase (Coulet method). [Color figure can be viewed in the online issue, which is available at wileyonlinelibrary.com.]

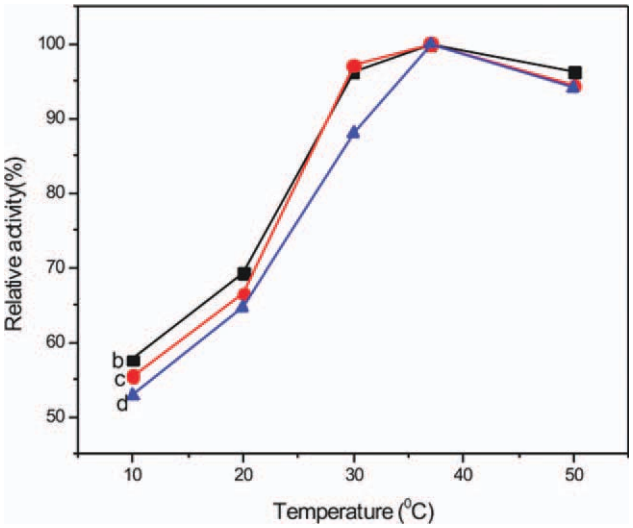

Figure 8 Variation of relative hydrolytic activity (%) with temperature: (b) PS–Hz–Glu–lipase, (c) PS–Glu–lipase, and (d) PS–Azo–lipase (Coulet method). [Color figure can be viewed in the online issue, which is available at wileyonlinelibrary.com.]

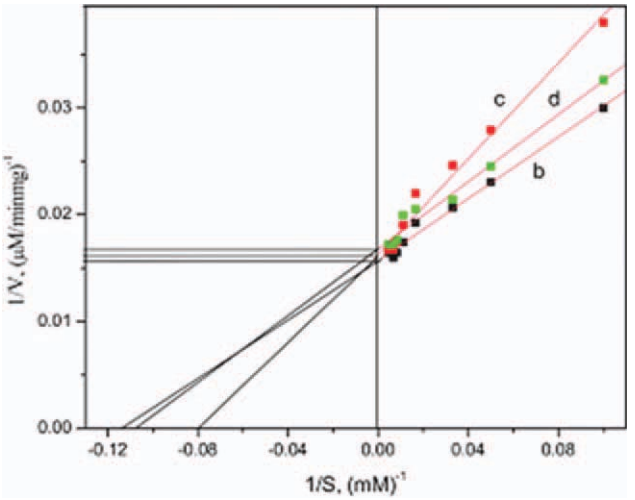

Figure 10 Lineweaver–Burk plot of the lipase-immobilized membranes for olive oil: (b) PS–Hz–Glu–lipase (R = 0.994), (c) PS–Glu–lipase (R = 0.989), and (d) PS–Azo–lipase (Coulet method; R = 0.989). [Color figure can be viewed in the online issue, which is available at wileyonlinelibrary.com.]

techniques. The immobilization reached a steady level at modified 5% AA grafted PS. Figure 4 shows the surface morphology of the Hz-modified, virgin, and lipase-immobilized membranes. The surface morphology of the Hz-modified membrane showed the particles spread over the membrane surface and showed marked differences from the embedded virgin PS membrane. The distinct protein aggregates on the membrane surface was visual proof of the immobilization of enzymes. Figure 5 shows the evidence of immobilization by X-ray diffraction (XRD). The peaks in the XRD pattern of the immobilized PS membranes showed that apart from peaks due to polyester fabric (inset II), there was another peak, and it was in conformity with the lipase powder peak (inset I) of the figure.

The reflection of pore-blocking behavior was evidenced from PWPs of the membranes at different modification stages. The normalized pattern of water permeability (with respect to the virgin membrane; Fig. 6) showed the reduction due to pore blocking of membranes in the modification process. It showed similar patterns for all of the AA-modified membranes. The normalized pattern of water permeability

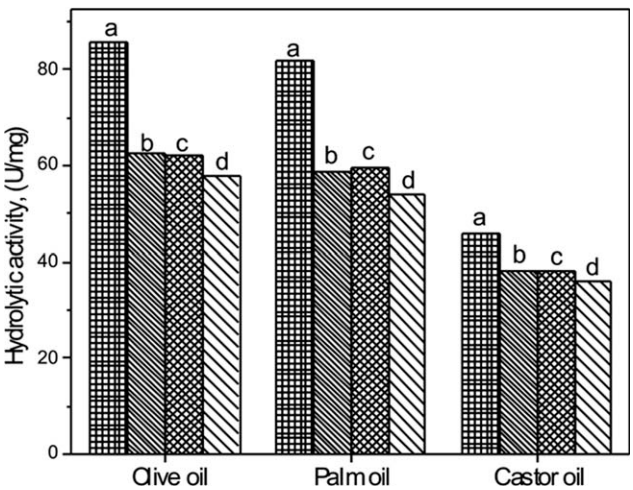

Figure 9 Hydrolytic activities of different lipase-immobilized membranes for different oils: (a) free lipase, (b) PS–Hz–Glu–lipase, (c) PS–Glu–lipase, and (d) PS–Azo–lipase (Coulet method).

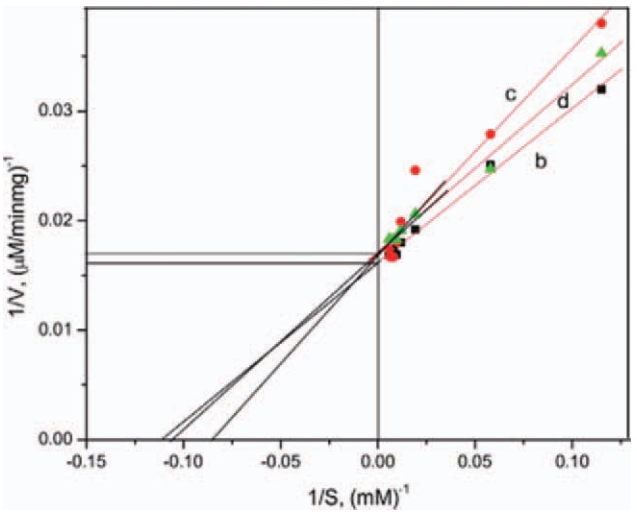

Figure 11 Lineweaver–Burk plot of the lipase-immobilized membranes for palm oil: (b) PS–Hz–Glu–lipase (R = 0.996), (c) PS–Glu–lipase (R = 0.970), and (d) PS–Azo–lipase (Coulet method; R = 0.994). [Color figure can be viewed in the online issue, which is available at wileyonlinelibrary.com.]

TABLE III
Kinetic Parameters of the Lipase Immobilized Membranes for Different Oil Substrates

Membrane	Olive oil		Palm oil		Castor oil	
	V_{max}	K_m	V_{max}	K_m	V_{max}	K_m
PS–Hz–Glu–lipase	64.5	8.69	62.5	9.09	41.6	18.86
PS–Glu–lipase	62.5	12.1	58.82	12.5	40.0	23.8
PS–Azo–lipase	60.6	9.43	58.82	9.25	40.0	19.6

(with respect to the virgin PS membrane) showed that AA grafting resulted in a distinct reduction compared to the other modification steps.

Comparison of the hydrolytic activities for different oils

Enzymatic hydrolysis of oils by lipases is the preferred method for the conversion of triglycerides into the constituent fatty acid and glycerol in the presence of water. As triglycerides are not dissolved in aqueous phase, the reactions have to take place at the interface of the water and oil phases.[38] As reported in our earlier publication,[32] the hydrolytic study of olive oil was done by a physically adsorbed lipase immobilized matrix, whereas in this study, it was done for the three oils (olive, palm, and castor oils) by an immobilized matrix covalently coupled and physically adsorbed

As pH affects the stability, structure, and function of many globular proteins because of their ability to influence electrostatic interactions, the extent of hydrolysis is different at different pHs. One determines the optimum pH for the hydrolytic reaction by conducting the reaction at different pH values (5–9). Figure 7 shows the variation of hydrolytic activities with pH for olive oil. The trend was the same for the other two oils (viz., palm and castor oils). The decline in enzyme activity in a pH profile near the optimum pH range was due to a reversible reaction that involved the ionization or deionization of acidic or basic groups in the active center of the enzyme protein.

Figure 8 shows the variation of the hydrolytic activities with temperature for olive oil. The enzyme-catalyzed reaction tended to proceed faster with increasing temperature, as kinetic energy. However, when the temperature of the enzyme-catalyzed reaction was raised still further, an optimum was reached. The trend was the same for the other two oils (viz., palm and castor oils). However, the heat denatured the enzyme, causing it to lose its three-dimensional functional shape, above the optimum temperature. The optimum pH and temperature were 8.0 and 37°C for hydrolysis of all three oils. Moreover, the modes of binding with the substrate did not reflect any change in terms of optimum pH and temperature.

Figure 9 depicts the yield of hydrolysis (U/mg) obtained for different oils with immobilized enzyme.

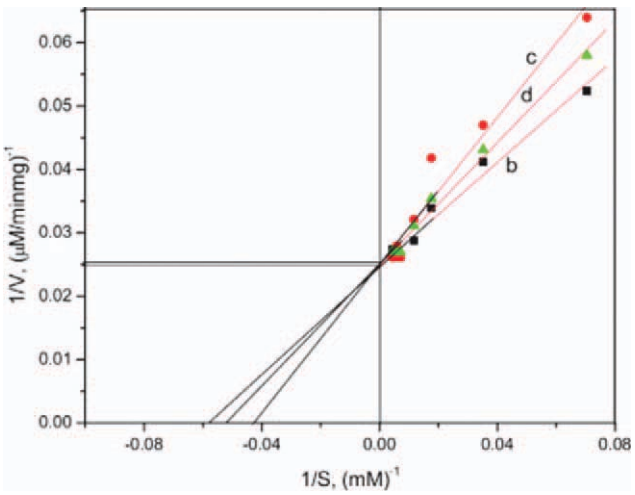

Figure 12 Lineweaver–Burk plot of the lipase-immobilized membranes for castor oil: (b) PS–Hz–Glu–lipase (R = 0.988), (c) PS–Glu–lipase (R = 0.975), and (d) PS–Azo–lipase (Coulet method; R = 0.994). [Color figure can be viewed in the online issue, which is available at wileyonlinelibrary.com.]

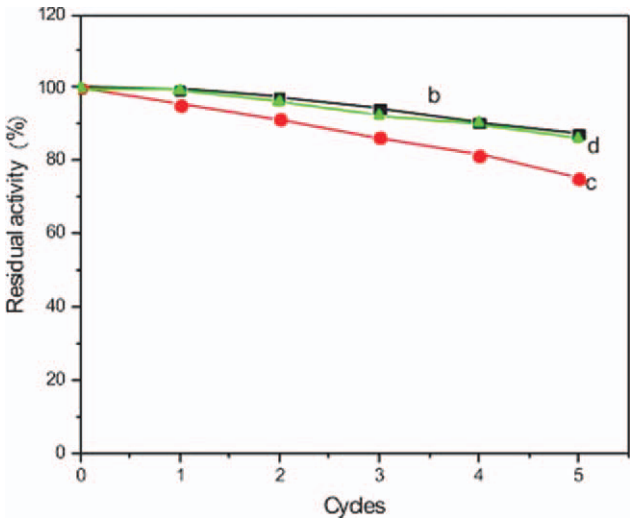

Figure 13 Reusability study of the lipase-immobilized membranes for olive oil: (b) PS–Hz–Glu–lipase, (c) PS–Glu–lipase, and (d) PS–Azo–lipase (Coulet method). [Color figure can be viewed in the online issue, which is available at wileyonlinelibrary.com.]

It shows that olive oil featured the highest yield compared to the other oils (palm and castor oils). The hydrolysis depended on the fitting of the chemical structure of the substrate with the enzyme, that is, the specificity of the structures. It was already established that *C. rugosa* lipase, with its L-shaped tunnel, was fitted for the recognition of the substrate chain, especially olive oil.[39] Castor oil was not appreciably hydrolyzed by free and immobilized lipases among the three oils. This slow rate of hydrolysis was also observed by Ibrahim and coworkers.[40,41] This could be explained by the structure of castor oil, in which ricinoleic acid was its main composition.

In the same figure, the hydrolysis extent is displayed according to the immobilizing method. The free lipase showed the maximum ability because of its easy accessibility toward the substrate. The Glu techniques (on the PS and Hz-modified surfaces) showed almost the same results. In both cases, the accessibility was same as for Glu crosslinked onto the surface. In the Coulet method, the microenvironment was different because of covalent attachment, and it was more restricted. Thus, the extent of hydrolysis was the lowest of all.

The lipase hydrolytic reaction with oils can be presented as follows

$$\text{Lipase} + \text{S} \rightarrow \text{Lipase} - \text{S} \rightarrow \text{Lipase} + \text{P}$$

It is assumed that the oil substrate (S) interacts with lipase to form an intermediate lipase substrate complex. Then, it converts the substrate into the end product (P) and simultaneously regenerates lipase.

The Micahaelis–Menten equation[42,43] fit the linear Lineweaver–Burk transformation, and it is as follows

$$\frac{1}{V} = \frac{1}{V_{\max}} + \frac{K_m}{V_{\max}[\text{S}]}$$

where K_m represents the Michaelis–Menten constant (mM), [S] is the substrate concentration (mM), and $V_{\max}$ is the maximum reaction rate (mM/min).

The double-reciprocal plot (Lineweaver–Burk plot) of the reaction rate was used to evaluate K_m and $V_{\max}$, the maximum rate of enzyme-mediated reaction where enzyme active sites are saturated with different oil substrates (Fig. 10, olive oil; Fig. 11, palm oil; Fig. 12, castor oil). As shown in Table III, the K_m value for castor oil was the maximum for all three immobilized lipases. This means that castor oil had the lowest affinity among the three oils considered here. The structural pattern (due to the presence of —OH functionality) did not fit well with the lipase. The —OH functionality of castor oil inhibited the fit of the add-on with the lipase (lock and key model). On the other hand, it possessed minimum $V_{\max}$ values. The glutraldehyde bridging lipase on the PS membrane surface showed the lowest affinity toward castor oil, as the K_m value (highest) suggests. This means that lipase binding over the PS membrane did not fit well (lock and key model) in the castor oil substrate, whereas the lipase immobilized over the aminated surface and the lipase immobilized by covalent approaches showed good affinities.

Reusability of the lipase-immobilized membranes

Although the immobilization of lipase facilitated reuse and retained its activity, repetitive use of the immobilized enzyme led to deactivation of the enzyme. The initial activity was considered 100% for all three membranes. The deterioration of activity (Fig. 13) of lipase on PS–Hz–Glu (12.5%) and PS–Azo (13.7%) showed similar behavior after five cycles, whereas the deterioration was comparatively greater for the PS–Glu (24.6%) membrane.

CONCLUSIONS

Different techniques of immobilization were carried out on virgin and Hz-modified asymmetric PS membranes. The Hz modification depended on the AA content. The PS–Hz–Glu membranes showed maximum lipase immobilizing capacity. The hydrolytic activities (U/mg) of the three oils were studied and showed the following trend: Olive oil (62.37) > Palm oil (58.9) > Castor oil (38.11). Actually, the ricinoleic acid in castor oil lowered the hydrolysis aptitude, which was proven by the highest K_m value (K_m = 18.86 mM). The $V_{\max}$ values also followed the trend for the same membrane: Olive oil (64.5 mM/min) > Palm oil (62.5 mM/min) > Castor oil (41.6 mM/min). The deterioration values of the activity of lipase were PS–Hz–Glu (12.5%), PS–Azo (13.7%), and PS–Glu (24.6%) after five cycles.

References

1. Hartmeier, W. Immobilized Biocatalysts; Springer-Verlag: Berlin, 1986.
2. Huang, X. L.; Catignani, G. L.; Swaisgood, H. E. J Biotechnol 1997, 53, 21.
3. Kise, H.; Hayakawa, A. Enzyme Microb Technol 1991, 13, 584.
4. Saleem, M.; Rashid, M. H.; Jabbar, A.; Perveen, R.; Khalid, A. M.; Rajoka, M. I. Process Biochem 2003, 40, 849.
5. Bhandari, S.; Gupta, V. K.; Singh, H. Biocatal Biotrans 2009, 27, 71.
6. Noinville, S.; Revault, M.; Baron, M.; Tiss, A.; Yapoudjian, S.; Ivanova, M. Biophys J 2002, 82, 2709.
7. Gao, S.; Wang, Y.; Wang, T.; Luo, G.; Dai, Y. Bioresour Tech 2009, 100, 996.
8. Serra, E.; Alfredsson, V.; Blanco, R. M.; Diaz, I. Stud Surf Sci Catal 2008, 174, 369.
9. Ghiaci, M.; Aghaei, H.; Soleimanian, S.; Sedaghat, M. E. Appl Clay Sci 2008, 43, 289.

10. Wang, Y.; Hu, Y.; Xu, J.; Luo, G.; Dai, Y. J Membr Sci 2007, 293, 133.
11. Bayramoglu, G.; Kacar, Y.; Denizli, A.; Arica, M. Y. J Food Eng 2002, 52, 367.
12. Hayes, D. J Am Oil Chem Soc 2004, 81, 1077.
13. Deng, H. T.; Xu, Z. K.; Dai, Z. W.; Jian, W.; Patrick, S. Enzyme Microb Technol 2005, 36, 996.
14. Monier, M.; El-Sokkary, A. M. A.; Sarhan, A. A. React Funct Polym 2010, 70, 122.
15. Rudnik, E.; Dobkowski, Z. J Therm Anal Calorim 1995, 45, 1153.
16. Peinemann, K. V.; NunesS. P. Membranes for Life Sciences; Wiley: Hoboken, NJ, 2008.
17. Kumar, Y.; Popat, K. M.; Brahmbhatt, H.; Ganguly, B.; Bhattacharya, A. J Hazard Mater 2008, 154, 426.
18. Saha, N. K.; Balakrishnan, M.; Ulbricht, M. Desalination 2009, 249, 1124.
19. Ciobanu, M.; Marin, L.; Cozan, V.; Bruma, M. Rev Adv Mater Sci 2009, 22, 89.
20. Radvanovic, P.; Thiel, S. W.; Hwang, S. T. J Membr Sci 1992, 65, 231.
21. Reinish, M. D. J Am Oil Chem Soc 1956, 33, 516.
22. Pryde, E. H. Fatty Acids; The American Oil Chemist's Society: Champaign, IL, 1985.
23. Brady, C.; Metcalfek, L.; Slaboszewski, D.; Frank, D. J Am Oil Chem Soc 1988, 65, 917.
24. Shinota, A.; Machida, H.; Azuma, T. (to Meito Sangyo Co., Ltd.). Jpn. Pat. 71:16,509 (1967).
25. Murty, V. R.; Bhat, J.; Muniswaran, P. K. A. Biotech Bioprocess Eng 2002, 7, 57.
26. Lakshminarayana, G.; Subbarao, R.; Sastry, Y. S. R.; Kale, V.; Rao, T. C.; Gangadhar, A. J Am Chem Soc 1984, 61, 1204.
27. Wikipedia. http://en.wikipedia.org/wiki/.
28. Kim, J. Y.; Lee, H. K.; Baik, K. J.; Kim, S. C. J Appl Polym Sci 1997, 65, 2643.
29. Yogesh, P. P.; Basu, S.; Bhattacharya, A. J Appl Polym Sci 2007, 105, 609.
30. Coulet, P. R.; Julliard, J. H.; Gautheron, D. C. Biotechnol Bioeng 1974, 16, 1055.
31. Lowry, O. H.; Rosebrough, N. J.; Farr, A. L.; Randall, R. J. J Biol Chem 1951, 193, 265.
32. Gupta, S.; Yogesh, J. S.; Bhambi, M.; Pundir, C.; Singh, K.; Bhattacharya, A. Int J Biol Macromol 2008, 42, 145.
33. Bhattacharya, A.; Ray, P.; Brahmbhatt, H.; Vyas, K. N.; Joshi, S. V.; Devmurari, C. V.; Trivedi, J. J. J Appl Polym Sci 2006, 102, 3575.
34. Reuvers, A. J.; Smolders, C. A. J Membr Sci 1987, 34, 67.
35. Cohen, C.; Tanny, G. B.; Prager, S. J Polym Sci Polym Phys Ed 1979, 17, 477.
36. Kang, Y. S.; Kim, H. J.; Kim, U. Y. J Membr Sci 1990, 60, 219.
37. Yamagishi, H.; Grivello, J. V.; Belfort, G. J Membr Sci 1995, 105, 237.
38. Pronk, W.; Kerkhof, P. J. A.; Helden, C.; Reit, V. K. Biotechnol Bioeng 1988, 32, 512.
39. Freitas, L.; Bueno, T.; Perez, V. H.; Santos, J. C.; de Castro, H. F. World J Microb Biotechnol 2007, 23, 1725.
40. Ibrahim, C. O.; Hayashiand, M.; Nagai, S. Agric Biol Chem 1987, 51, 37.
41. Moskowitz, G. J.; Cassaigne, R.; West, I. R.; Shen, T.; Feldman, L. I. J Agric Food Chem 1977, 25, 1146.
42. Gupta, S.; Singh, K.; Bhattacharya, A. Int J Biol Macromol 2010, 46, 445.
43. Lineweaver, H.; Burk, D. J Am Chem Soc 1934, 56, 658.